

# Performance Study and Energy Saving Mechanism Analysis of an Absorption/mechanical Hybrid Heat Pump Cycle

Na Zhang<sup>a,\*</sup>, Kang Wang<sup>a,b</sup>, Noam Lior<sup>c</sup>, Wei Han<sup>a</sup>

<sup>a</sup> Institute of Engineering Thermophysics, Chinese Academy of Sciences, Beijing 100190, China.

<sup>b</sup> Graduate University of the Chinese Academy of Sciences, Beijing 100049, China.

<sup>c</sup> University of Pennsylvania, Department of Mechanical Engineering and Applied Mechanics, Philadelphia, PA  
19104-6315, USA

\* Professor, PhD, Institute of Engineering Thermophysics, Chinese Academy of Sciences, [zhangna@iet.cn](mailto:zhangna@iet.cn)

## Abstract:

A hybrid heat pump cycle of the heat amplifier type integrating a booster compressor between the generator and the condenser for distributed heating is simulated and analyzed. The interrelation between the two sub-cycles and the hybridization principle are explored. The theoretical analysis is demonstrated by a H<sub>2</sub>O/LiBr based hybrid cycle simulation.

Investigation of the interaction mechanisms between the mechanical compression and absorption has shown that there is an optimal compression ratio of about 1.2-1.8 for which the low-temperature driving heat can be utilized most effectively (giving highest coefficients of performance). A study was also carried out to reveal the energy saving mechanism in the hybrid system as compared with an individual absorption heat pump and a simple vapor compression heat pump working within the same temperature regions. The results indicate that replacement of a part of the mechanical work with low-grade heat makes the hybrid cycle achieves not only significant energy saving of high-quality mechanical work, but also better use of low-grade waste heat because of the cascade use of the two energy inputs. The coefficient of performance (based on both power and heat input) and heat driving coefficient of performance in the hybrid cycle are found to be improved by 10.2% and 16.6%, respectively, in comparison with separate absorption and vapor compression systems.

## Keywords:

low-grade heat, energy saving mechanism, hybrid heat pump cycle, thermodynamic performance, ultimate temperature lift.

## 1. Introduction

The absorption cycle [1] has the potential of low-temperature waste heat recovery for refrigeration/cooling or heating applications, and its performance can be improved by integration with a mechanical compression process driven by a small fraction of mechanical work, such hybridization is called absorption-compression hybrid cycle [2].

Boer et al. have analyzed a hybrid refrigeration cycle that includes a low-pressure compressor positioned between the evaporator and the absorber [3]. For a constant evaporation temperature, they stated that it can either increase the absorption temperature or reduce the generation temperature. On the other hand, for a constant absorption temperature, it achieves a reduced evaporation temperature for higher quality (lower temperature) refrigeration production. Kim et al. proposed the integration of a compressor in an H<sub>2</sub>O/LiBr-based triple-effect absorption cooling system to avoid the corrosion problem caused by the high generator temperature [4], and found that the resulting generator temperature decrement increases with elevated compression ratios, and that a 40 K generator temperature decrement can be obtained at the cost of 3-5% cooling-capacity-equivalent power input for driving the compressor.

For a given condensation temperature, a high-pressure-side compressor between the generator and the condenser lowers the generator pressure and accordingly its temperature, thus favouring external low-temperature heat recovery. Alternatively, for a constant generation temperature, it increases the condensation temperature, enabling heat production from the heat of condensation. Hybrid cycles of the heat amplifier type using the ammonia/water working pair were simulated in [5], and confirmed their capability of utilization waste heat for cooling and heating mode with a high level of efficiency. In addition to the basic configurations, some new cycle configurations were also proposed for further improving the hybrid cycle performance [6-8].

Most of the past research focused mainly on case studies with parametric analysis and selection of working solutions, Zheng and Meng tried first to explore the energy saving mechanism of the hybrid refrigeration cycle with a low-pressure side compressor, by studying the thermodynamic ultimate state and exploring the potential of lowering evaporation temperature [9, 10]. It was concluded that the two sub-cycles compete in their contribution to the hybrid refrigeration system, and there is an optimal compressor outlet pressure region under specified working conditions.

In this paper, a hybrid heat pump cycle of the heat-amplifier type integrating a booster compressor between the generator and the condenser for distributed heating is simulated and analyzed. A high-pressure-side compressor is incorporated, which consumes more mechanical power for the same pressure ratio due to the higher inlet temperature, but at the same time offers an advantage of smaller size because of the reduced specific volume of refrigerant vapour. The interaction mechanisms between the mechanical compression and thermal compression was investigated to find the effect of the compressor compression ratio on the effectiveness of low-temperature driving heat use that would result in the highest coefficients of performance (*COP*). To explore thermodynamic performance and the energy saving mechanisms of the hybrid cycle, a comparison study was also conducted among the hybrid cycle, the conventional vapor compression cycle, and the absorption heat pump cycle working within the same temperature regions.

## 2. The absorption heat amplifier (AHA) cycle and its ultimate temperature lift conditions

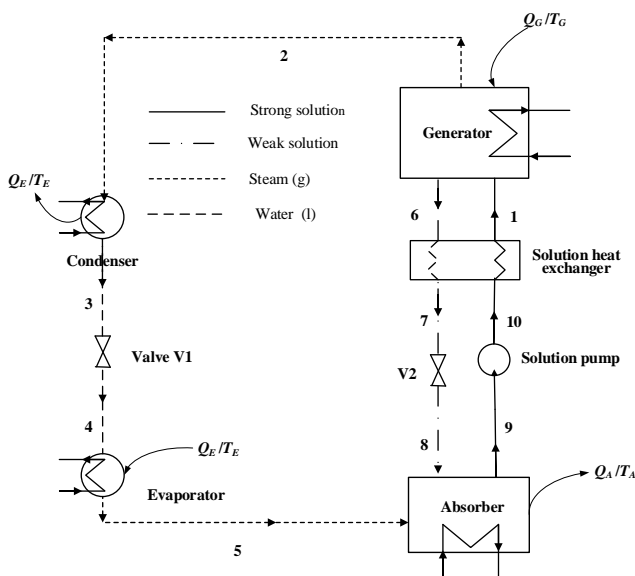


**Fig. 1 Schematic diagram of the absorption heat amplifier AHA cycle**

The single effect absorption heat amplifier (AHA) cycle (Fig.1) consists of a generator, condenser, evaporator and absorber, solution pump, heat exchanger, and throttling valves. Taking advantage of the large boiling point difference between the refrigerant and the absorbent, the loops of refrigerant (1→2→3→4→5) and of solution (1→6→7→8→9→10→1) are formed; they separate in the generator and join together in the absorber. By arranging generation and condensation at a higher pressure, and evaporation and absorption at a lower pressure, the cycle has two pressure levels and three temperature levels (assuming  $T_A = T_C$ ). Driven by the higher-temperature ( $T_G$ ) waste heat  $Q_G$  in the generator, it takes

lower-temperature ( $T_E$ ) heat  $Q_E$  in the evaporator and upgrades it, and delivers mid-temperature ( $T_C$ ) heat  $Q_C$  and  $Q_A$  in the condenser and absorber.

The cycle coefficient of performance ( $COP_0$ ) is thus defined as:

$$COP_0 = \frac{Q_C + Q_A}{Q_G} \quad (1)$$

which expresses the specific heat production per unit heat input at  $T_G$ , for the heat amplifier cycle,  $COP_0 \geq 1$ . There exists an internal restriction between the specific heat production  $COP_0$  and its delivery temperature  $T_C$ . For given heat source and sink temperatures ( $T_G$  and  $T_E$ ), the higher the delivery temperature  $T_C$  is, the lower the specific heat production  $COP_0$  will be.

The basic working principle of the AHA cycle can be explained by a  $\log P$ - $T$  diagram, as shown in Fig. 2. Aiming at heat movement from the higher- and lower-temperature levels to the mid-temperature level, the evaporation/condensation of the refrigerant and the absorption/desorption of the refrigerant with the absorbent occur at low-/high-pressure levels, forming the refrigerant loop  $G_i C E A G_i$  and the solution loop  $G_i G A_i A G_i$ , respectively. Each state point is positioned based on its pressure and temperature. In addition, from the left to the right, the refrigerant concentration decreases for the phase equilibrium lines ( $x_r > x_s > x_w$ ).  $\Delta x$  represents the concentration difference between the strong solution and the weak solution.

For heat production at a higher temperature ( $T'_C > T_C$ ) level, the condensation pressure needs to be elevated. As shown in Fig. 2, under given heat source conditions ( $T_G/P_G$ , and  $T_E/P_E$ ), the condensation isobar line thus moves up from  $P_C$  to  $P'_C$ , it intersects the extension of  $CE$  at point  $C'$ ,

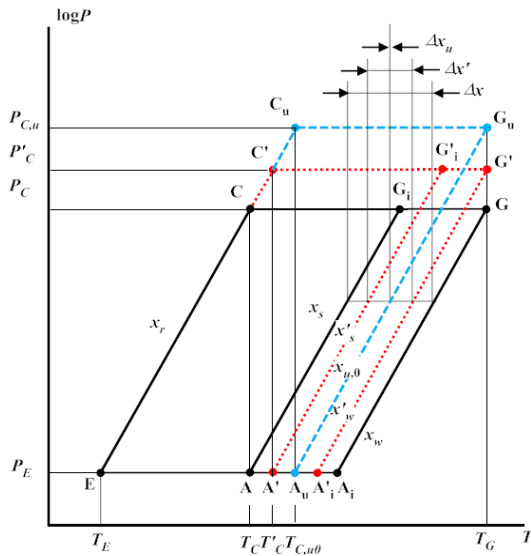


**Fig. 2**  $\log P$ - $T$  diagram of the AHA cycle

it intersects the extension of  $CE$  at point  $C'$ , and intersects the isothermal line of  $T_G$  at point  $G'$ . Keeping  $T'_A = T'_C$ , another absorption cycle  $G'_i C' E A' G'_i - G'_i G' A'_i A' G'_i$  is formed, in which the heating supply temperature is increased to  $T'_C$ , and at the same time the solution concentration difference drops to  $\Delta x'$ . Following the same procedure, along with the increasing condensation pressure, a series new absorption cycles will be formed with continuous drop of  $\Delta x$  and increase of temperature lift ( $\Delta T = T_C - T_E$ ). Increasing the condensation pressure until it reaches  $P_{C,u}$ , an ultimate absorption cycle will eventually be reached as  $G_u C_u E A_u G_u$ , in which  $\Delta x_u = 0$ . Correspondingly the temperature lift is maximal for given  $T_G$ ,  $\Delta T_{u0} =$

$T_{C,u0} - T_E$ . This ultimate cycle is impractical since the driving force  $\Delta x$  of the absorption process drops to 0, thus no absorption occurs, and it loses the ability of heat amplification with

$$COP_u = \lim_{\Delta x \rightarrow 0} COP = 1.$$

### 3. The hybrid absorption compression heat amplifier (ACHA) system and its simulation

#### 3.1 The hybrid ACHA system description

When the single effect absorption heat amplifier cycle is unable to meet the desired heat production requirement, a common solution is to devise and implement combined cycles, either multi-effect absorption cycles by combining several absorption cycles (which demands higher-temperature driving heat input), or hybrid cycles by integrating mechanical compression into the absorption cycle.

A hybrid absorption-compression heat amplifier (ACHA) cycle with series connection of the thermal compression and mechanical compression is shown in Fig. 3. A booster compressor is employed here between the generator and the condenser,

thus adding one more operational option to the hybrid cycle: it enables condensation to occur at a pressure higher than that of generation. The pressure rise in the hybrid cycle is thus accomplished by thermal compression and a succeeding mechanical compression in a relay. As the compression ratio increases, the fraction of mechanical compression increases, leading to corresponding changes in the operating parameters and performance of both the thermal and mechanical compression because of their interactions.

#### 3.2 The thermodynamic model and its validation

The lithium bromide aqueous solution ( $\text{H}_2\text{O-LiBr}$ ) is commonly employed for absorption air-conditioning purposes because of its favorable operation conditions for evaporation temperature  $> 5^\circ\text{C}$ . The large boiling point difference between LiBr ( $1265^\circ\text{C}$  under atmospheric pressure) and  $\text{H}_2\text{O}$  eliminates the need for rectification. A comparison in [3] of 4 different working fluid pairs in single-effect absorption cycles concluded that the classical working pairs including  $\text{H}_2\text{O-LiBr}$  and  $\text{NH}_3\text{-H}_2\text{O}$  offer the best combination of high vaporization enthalpy of the refrigerant fluid and low solution circulation ratio. This working fluid pair is therefore selected as the absorption working fluid in this paper because of its proven performance for the aimed temperature region application and easy availability. The drawbacks of this working pair are the limitation of the working range due to freezing point of water and crystallization, its corrosivity for the metal components of the machine at temperatures above  $200^\circ\text{C}$  [4], and the large compressor size due to the large specific volume of water vapour. The latter can be at least partially alleviated by incorporating the compressor at the high-pressure side. Solar or industrial waste heat at 135 to  $150^\circ\text{C}$  can be used, for example, as the driving heat sources.

Some assumptions for cycle simulation are:

- (1) Steady-state operation;

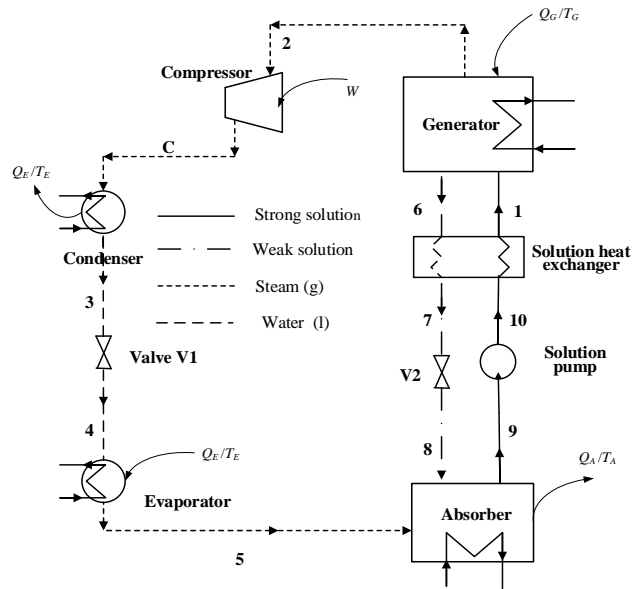


Fig. 3 Schematic diagram of the hybrid ACHA cycle

- (2) The pressure losses in the generator, condenser, evaporator and absorber are 3% of the inlet pressure;
- (3) Expansion through the throttle valve is isenthalpic;
- (4) Heat losses to the ambient are ignored;
- (5) The outflow solutions of the generator and absorber are at saturated states.
- (6) The outlet temperatures of the absorber and condenser are set to be equal,  $T_C = T_A$ .

Other major equipment specifications used in the simulation are listed in Table 1.

*Table 1. Specified simulation parameters of major equipment*

Item	Value
Minimum temperature difference in SHX, /°C	5
Pump efficiency	0.7
Compressor isentropic efficiency	0.72
Mass fraction of the H <sub>2</sub> O in the refrigerant	1

The systems are simulated with the Aspen Plus process simulation software [11], in which the component models are based on the energy balance and mass balance and species balance, with the default relative convergence error tolerance of 0.01%, which is the specified tolerance for all tear convergence variables. The working fluid thermal properties are calculated with the ELECNRTL for the binary solution and the STEAM - TA for water and steam, respectively. The generator is simulated with the “Flash/Separators” module, and the absorber with the “Mixer/Heater” module. To validate the simulation model, the VLE (Vapor-Liquid equilibrium) data are compared with those in [12], showing that the largest relative error is 6.93%, and that the average relative error is no more than 2.50%.

### 3.3 Evaluation criteria

The coefficient of performance (*COP*) based on the first law of thermodynamics is defined as:

$$COP_0 = \frac{Q_C + Q_A}{Q_G + W} \quad (2)$$

This definition is for both the absorption cycle (with  $W$  being the pump power consumption) and the hybrid cycle (with  $W$  being the sum of the pump and compressor power consumptions).

Since the two energy inputs, mechanical work  $W$  and the generator heat input  $Q_G$  e, are very different in terms of their energy quality, especially when low-temperature heat or solar heat are used as the heat source, a more proper accounting for the contribution of the low-temperature heat input, the following heat driving coefficient of performance (*COP*), following [9, 10] is defined as:

$$COP = \frac{Q_C + Q_A - W \cdot COP_w}{Q_G} \quad (3)$$

Where  $COP_w$  is the coefficient of performance of a vapor compression heat pump cycle operating at the same evaporation and condensation temperatures as those of the hybrid one. The definition of *COP* in Eq. (3) signifies the driving effect of low-temperature heat in the hybrid cycle, and makes it possible to compare the performance between cycles with different configurations and parameters.

## 4. Discussion of System Performance and Hybridization Mechanisms

### 4.1 Performance of the AHA cycle

With lithium bromide aqueous solution ( $\text{H}_2\text{O-LiBr}$ ) as the working solution, Fig. 4 shows the variation of the heat-driving  $COP$ , the corresponding concentration difference  $\Delta x$  and cycle circulation ratio  $CR$  (the ratio of the strong solution mass flow rate over the refrigerant mass flow rate) for the AHA cycle at given  $T_E=30^\circ\text{C}$  and  $T_G=140, 145$  and  $150^\circ\text{C}$ . In Fig. 4, the ultimate heat delivery temperature  $T_{C,u}$  and thus ultimate temperature lift  $\Delta T_u$  can be identified for each given pair of  $T_E$  and  $T_G$ . It is found that  $\Delta T_u$  increases with  $T_G$ . When  $T_G$  increases from  $140^\circ\text{C}$  to  $150^\circ\text{C}$  for example,  $\Delta T_u$  increases from  $48^\circ\text{C}$  to  $53^\circ\text{C}$ . At the ultimate state, the corresponding solution concentration difference drops to 0, and the heat amplifier has the worst performance of zero function with  $COP = 1$ . The above observation validates the quantitative analysis in Section 2. It is also found that the cycle circulation ratio increases to infinity at the ultimate state, similar to the observation [9] that analyzes an absorption refrigeration cycle. As the AHA cycle starts to deviate from the ultimate state, the solution concentration difference increase continuously, and the circulation ratio  $CR$  first drops sharply and after some turning point it drops very mildly. In correspondence to the variation of  $CR$ , the cycle  $COP$  first increase quickly and then ascends much more gently, suggesting that the performance of the AHA cycle is mainly affected by  $CR$  and gets deteriorated quickly at high  $CR$ .

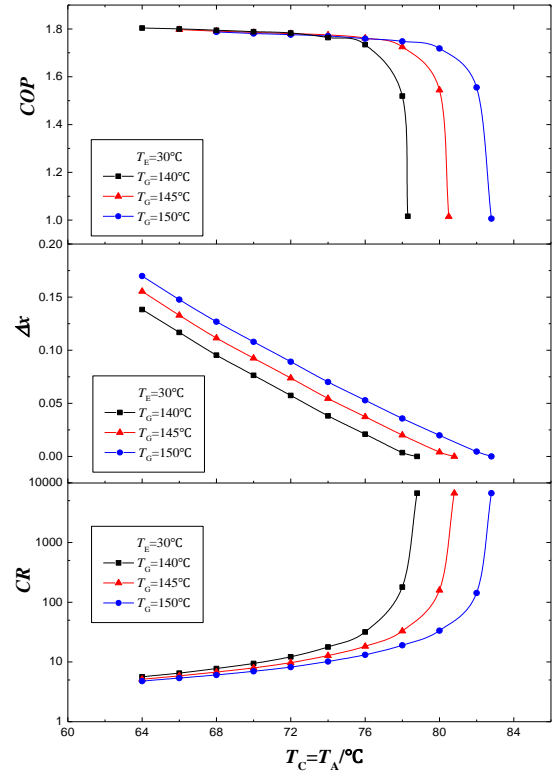


Fig.4 Variation of  $COP$ ,  $\Delta x$  and  $CR$  in the AHA cycle

### 4.2 Hybridization scheme and principle

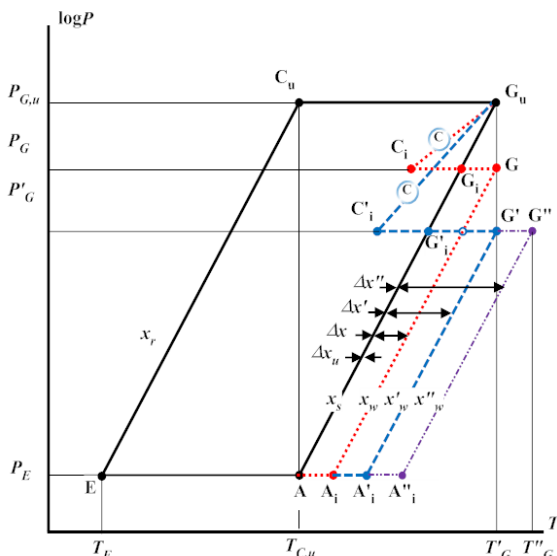


Fig. 5  $\log P$ - $T$  diagram of the hybrid cycle with reduced generation temperature

For given high- and low-temperature heat sources temperatures ( $T_G$  and  $T_E$  ( $P_E$ )), and given heat production pressure/temperature, adding a compressor at the high pressure side allows the generator to run under a lower pressure.

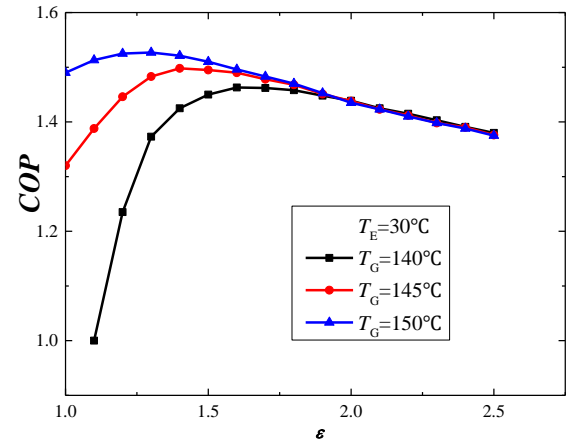
The ultimate absorption cycle for given  $T_E$  and  $T_G$  is shown as the path  $G_u C_u E A G_u$  in Fig. 5 in which there is no heat amplification effect since  $\Delta x = 0$  and  $CR = \infty$ . By introducing a compressor between the generator and the condenser, a hybrid cycle  $G_i C_i G_u C_u E A G_i / G_i G A_i A G_i$  is formed in which the generation pressure drops from  $P_{G,u}$  to  $P_G$ . For constant  $T_G$ , the weak solution concentration

decreases to  $x_w$  while the strong solution concentration  $x_s$  remains the same, thus leading to the increase of the concentration difference from  $\Delta x_u$  to  $\Delta x$ , and a corresponding drop of  $CR$ , where the thermal compression becomes feasible. As the generation pressure deviates from the ultimate value, Fig. 4 shows that the performance of the thermal compression becomes improved significantly at first and then more mildly. The hybridization therefore enables a heat amplification effect at  $T_{C,u}$  without increasing the low-grade heat temperature  $T_G$ . Further increase of the compression ratio causes the generation pressure to drop to  $P'_G$ , thus forming a new hybrid cycle with a higher concentration difference,  $\Delta x' > \Delta x > \Delta x_u$ . Increasing the compression ratio thus creates a series of new hybrid cycles with continuously dropping generation pressure, increasing concentration difference, and decreasing  $CR$ .

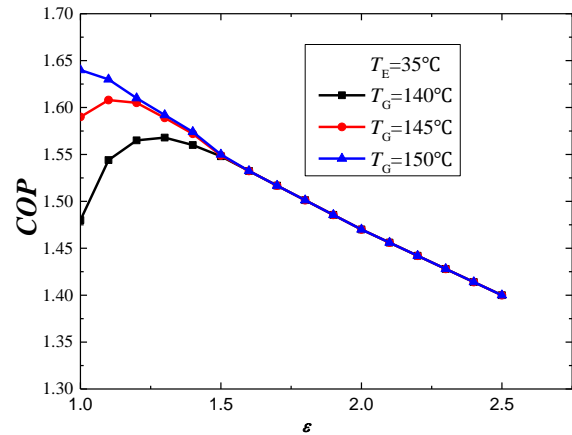
Theoretically, the compressor inlet pressure (which equals to  $P_G$ ) can be varied between given  $P_C$  and  $P_E$ . Especially, when the compression ratio  $\varepsilon = 1$  ( $P_G = P_C$ ), the hybrid cycle degrades into an absorption cycle; and when  $\varepsilon = P_C/P_E$ , ( $P_G = P_E$ ), the hybrid cycle becomes a pure mechanical compression one. Along with the increase of the compression ratio, the fraction of mechanical compression increases, leading to the steady increase of the compression work, while the thermal compression performance follows the pattern described in Fig. 4, it deviates away from the ultimate state and exhibits changes in response to the variation of  $CR$ . Apparently, at the lower compression ratio region, the rapid increase of the thermal compression performance overrides the steady increase of the compression work consumption, and the hybrid cycle  $COP$  increases accordingly. After reaching a certain pressure ratio, the gain in the thermal compression performance becomes more gradual so it cannot make up the rise in compression work demand, thus causing a drop in the hybrid cycle  $COP$ . It can thus be concluded that there exists an optimal pressure ratio at which a compromise is arrived between the thermal compression and the mechanical compression, and the hybrid cycle performance reaches the optimum for given  $T_E$  and  $T_C$ . Figure 5 also shows the influence of the generation temperature: for a given generation pressure  $P'_G$ , in correspondence to the increase of the generation temperature from  $T'_G$  to  $T''_G$ , the concentration difference increases further from  $\Delta x'$  to  $\Delta x''$ .

A hybrid cycle with  $H_2O/LiBr$  as the working fluid is simulated to validate the preceding results and their discussion. Figure 6 shows the influence of the compression ratio on the hybrid cycle performance for the given heat delivery temperature of  $T_A = T_C = 80^\circ C$  and  $x_s = 0.376$ . The generation temperature is varied between  $140^\circ C$  and  $150^\circ C$  in  $5^\circ C$  steps, the evaporation temperatures are chosen to be  $30^\circ C$  and  $35^\circ C$ .

It shows the existence of an optimal compression ratio  $\varepsilon_{opt}$  for each given  $T_G$ . The maximal  $COP$



(a)  $T_E=30^\circ C$



(b)  $T_E=35^\circ C$

**Fig.6. Influence of compression ratio in the hybrid cycle ( $T_C = T_A = 80^\circ C$ )**

increases as  $T_G$  is raised, while the corresponding  $\varepsilon_{opt}$  decreases. For example, when  $T_G$  is raised from 140°C to 150°C, the maximal  $COP$  increase from 1.46 to 1.53, and the optimal pressure ratio drops from 1.57 to 1.23. For the same pressure ratio, higher  $T_G$  not only enhances the refrigerant vaporization but also raises the solution concentration difference, thus favors heat generation. Driven by the increase of both pressure ratio and  $T_G$ ,  $\Delta x$  increases more rapidly, and the optimal  $COP$  is reached at a lower pressure ratio.

Comparing Figs. 6a and 6b, it is found that increase of the evaporation temperature  $T_E$  has an effect similar to that of raising  $T_G$ . When  $T_E$  increases from 30°C to 35°C, the maximal  $COP$  increases, while the optimal pressure ratio drops. It is because when  $T_E$  increases, the evaporation pressure increases as well, leading to the reduction of the total compression requirement, thus the fraction of mechanical compression reaches a higher level although the absolute compression ratio is still low.

## 5. System comparison and energy saving mechanism

### 5.1 System comparison

A typical hybrid ACHA cycle is simulated under the conditions of  $T_G=145^\circ\text{C}$ ,  $T_E=30^\circ\text{C}$  and  $T_C=80^\circ\text{C}$  with corresponding compression ratio of  $\varepsilon = 1.5$  and compressor outlet pressure  $P_{out} = 47.4$  kPa. The strong solution (in respect of the refrigerant) concentration  $x_r = 0.376$  kg/kg. Other related assumptions are summarized in Table 1.

The parameters of the major state points in the hybrid cycle are listed in Table 2. For comparison, an absorption heat amplifier cycle with the same working solution and a compression heat pump cycle with  $\text{H}_2\text{O}$  as working fluid are also simulated. It should be pointed out that it is very impractical to use  $\text{H}_2\text{O}$  for a compression heat pump due to the large specific volume of water vapor, and this hypothetical cycle is simulated only for thermodynamic performance comparison. The separate systems are assumed to operate at steady state and under the same assumption as the hybrid cycle. The results are summarized in Table 3.

The comparison absorption heat pump has a  $COP$  of 1.29, while the CHP cycle has a much higher performance, of  $COP = 4.5$ . As compared with the two individual systems with the same heat input from the higher-temperature heat source and electricity input, the hybrid system produces more mid-temperature heat, 38.1 kW as compared to 33.1 kW in the individual systems. The output difference comes from the different heat amount taken from the low-temperature heat source. The hybrid system takes 14.2 kW low-temperature heat at 30°C and upgrades it to 80°C for useful output, which is more than double the amount in the individual AHA cycle. The low-temperature heat contribution to the total heat input is < 22.5% in the absorption heat amplifier cycle, and > 38% in the hybrid system, all at an energy expense of only 3% electricity input (relative to the generator heat input).

If compared with the CHP cycle which has a much higher  $COP$ , the hybrid cycle produces more heat for the same electricity consumption (38.1 kW vs. 3.2 kW), attributed to the contribution of the low-temperature waste heat. Based on the data in Table 3, the electricity consumption in the hybrid cycle is 0.73 kW to produce 38.1 kW heat at 80°C. To produce the same amount of heat, the electricity consumption in the CHP cycle will have to be increased to 8.7 kW. The mechanical work saving ratio of the hybrid cycle is 92%. The hybrid cycle has therefore improved ability to use and upgrade low-temperature heat as compared with either individual cycle, and achieves energy saving



with  $COP_0$  and  $COP$  higher by 10.2% and 16.6%, respectively, as compared to the sum of the two individual systems.

Table 2. Hybrid cycle state point parameters

Stream	$T$ (°C)	$P$ (kPa)	Vapor fraction	Mass flow rate (kg/s)	Mass fraction	
					LiBr	H <sub>2</sub> O
1	108.5	32.1	0	1	0.642	0.358
2	145	31.6	1	0.064	0	1
C	204.2	47.4	1	0.064	0	1
3	80	46.8	0	0.064	0	1
4	30	4.2	0.086	0.064	0	1
5	29.4	4.1	1	0.064	0	1
6	145	31.6	0	0.936	0.686	0.314
7	113.5	31.4	0	0.936	0.686	0.314
8	95.3	4.2	0.018	0.936	0.686	0.314
9	80	4	0	1	0.642	0.358
10	80.1	3.21	0	1	0.642	0.358

Table 3. Performance comparison between the hybrid and individual systems

Item	Hybrid	Individual systems			Relative increase %		
		AHA	CHP	Total*			
Input	$Q_G$ kW (145°C)	23.15	23.15	\	23.15	\	
	$W$ kW	0.73	0.73	0.73	0.73	\	
	$Q_E$ kW (30°C)	14.22	6.71	2.57	9.98	14.22	\
Output	$Q_C + Q_A$ kW (80°C)	38.1	29.91	3.20	33.11	38.1	\
	$COP_0$	1.598	1.290	4.479	1.389	10.15	
	$COP$	1.507	\	\	1.290	16.59	

\*The sum from the two individual systems

## 5.2 Analysis of energy saving mechanism

Increasing the temperature lift  $\Delta T$  causes the  $COP$  to drop for both individual absorption and vapour compression heat pump cycles in their different patterns. The vapour compression cycle has a much higher performance, but its  $COP$  also drops more quickly with the increase of the compression ratio. In contrast, the  $COP$  of the absorption cycle exhibits a relatively mild variation, except the dramatic change near its ultimate state. When integrated into a hybrid cycle, an interrelationship between them has been established: as the compressor compression ratio increases, the fraction of the mechanical compression increases while that of the thermal compression drops, leading to the continuous evolution of the parameters and performance of both sub-cycles and their interrelation.

Based on the understanding of the performance of the absorption heat amplifier and the vapour compression heat pump, the energy saving mechanism is discussed with the help of log  $P$ - $h$  diagram (Fig. 7). The parameters of each state point are from the simulation results described in Section 5.1. The AHA cycle is also included for comparison, for the same evaporation (30°C/4.2 kPa) and

condensation (80°C/46.8 kPa) parameters values.

Fig.7 describes the diagrams of  $\log p$ - $T$  of the hybrid (solid line) and absorption heat amplifier AHA cycle (dotted line). The two cycles share the same parameters for the condensation and evaporation processes (represented by path 4-5-6), and the same strong solution concentration and mass flow rate. Main differences exist for the absorption (paths 5/8-9 for hybrid vs. 5/8a-9 for AHA) and generation processes (paths 1-2/6 for hybrid and 1a-2a/6a for AHA) due to additional pressure level of 31.6 kPa for the generation process in the hybrid cycle. Therefore in the hybrid cycle, the compression pressure elevation from  $P_E$  to  $P_C$  is accomplished by a cascade of the thermal compression (path 9-1) and mechanical compression (path 2-C), as compared with the thermal compression alone (path 8a-1a) in the AHA cycle. From the left to the right, there are 3 phase equilibrium lines with decreasing refrigerant mass concentration ( $x_r$ ,  $x_s$  and  $x_w$ , respectively), and they are 1.0, 0.358, and 0.315, for the hybrid cycle; and 1.0, 0.358 and 0.344 for the AHA cycle. The  $x_w$  line for the hybrid cycle is on the right of that for the AHA cycle, i.e.,  $x_w$  is lower for the hybrid cycle, despite the same generation temperature of 145°C in both cycles ( $T_2 = T_{2a}$ ). For the same strong solution concentration, lower  $x_w$  indicates more refrigerant is vaporized in the generation process, leading to more heat obtained from the evaporator and more heat delivery.

As mentioned, there exists an internal restriction between the heat production and its temperature lift  $\Delta T$  in the absorption heat amplifier cycle. Higher temperature lift lowers the heat production. By sharing the compression with a mechanical process, the temperature lift of the thermal compression drops as the compressor compression ratio increases, thus it has higher heat production than that in the pure AHA cycle, and the increment comes from the lower-temperature heat source via the evaporation process. At the same time, the performance of the mechanical compression drops but very importantly is still within the high  $COP$  region. This explains how a small fraction of mechanical compression helps improve the thermal compression performance. The core is the balance of the gain from the absorption side and the performance deterioration in the mechanical side, and thus the objective is to maximize the enhancement of low-temperature heat absorption for the least input of mechanical work, by cascade use of the two energy inputs. It is concluded that the hybrid cycle enhances the low-temperature thermal compression performance to a level which can't be achieved by an individual absorption heat pump cycle.

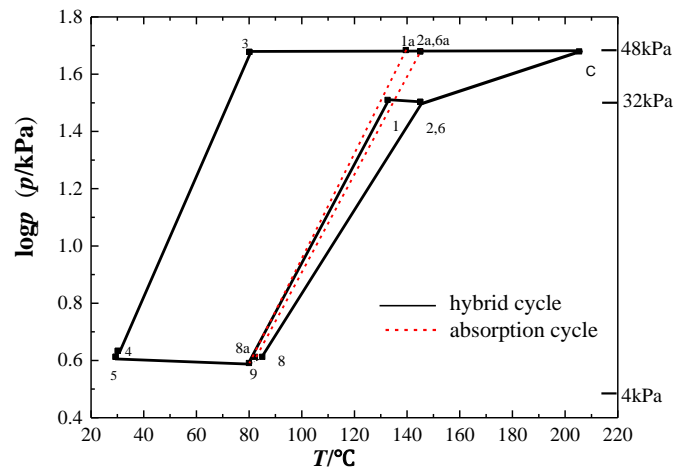


**Fig.7 Hybrid and absorption heat pump cycle comparison**

## 6. Conclusions

The absorption-compression hybrid cycle of heat-amplifier type was studied, focused on a hybridization principle based on the interrelation between the two sub-cycles, and the resulting energy saving mechanisms were analyzed. The theoretical analysis was validated by a simulation of a hybrid cycle working with H<sub>2</sub>O/LiBr solution.

The compression in the hybrid cycle can be regarded as a combination of mechanical compression

and thermal compression. The interrelation between the two sub-cycles determines the hybrid cycle performance and the existence of an optimal compressor compression ratio of 1.2~1.8.

To explore the thermodynamic performance and the energy saving mechanism of the hybrid system, a comparison was also conducted with a conventional absorption heat amplifier and a vapor compression heat pump cycle working within the same temperature regions. With the help of a small fraction of mechanical work (<5% to the waste heat input to the generator), the hybrid cycle accepts much more heat from the lower-temperature heat source than does the absorption heat amplifier cycle, and upgrades it to useful output. If compared with the vapor compression cycle which has a much higher  $COP$ , the hybrid cycle produces more heat for the same electricity consumption, attributed to the contribution of the low-temperature waste heat. The mechanical work saving ratio reaches up to 92%. The hybrid cycle has therefore improved ability to use and upgrade low-temperature heat, and achieves energy saving exhibited by  $COP_0$  and  $COP$  higher by 10.2% and 16.6%, respectively, as compared to the sum of the two individual systems.

It was concluded that the hybrid cycle achieves significant energy saving of high-quality mechanical work, and also improves the low-temperature thermal compression performance to a level which can't be achieved in an individual absorption heat pump cycle, i.e., it achieves simultaneously the better use of low-grade waste heat and energy saving of mechanical work, both attributed to the thermodynamically efficient cascade use to two energy inputs.

## Acknowledgments

The authors gratefully acknowledge support of the National Key Fundamental Research Project of China (No. 2013CB228302; No.2014CB249202)

## Nomenclature

ACHA	Hybrid absorption-compression heat amplifier cycle
AHA	Absorption heat amplifier cycle
CHP	Compression heat pump
$COP$	Coefficient of performance, dimensionless
$CR$	Cycle circulation ratio, dimensionless
$m$	Mass flow rate, kg/s
$P$	Pressure, kPa
$Q$	Heat duty, kW
$T$	Temperature, °C
$W$	Power consumption, kW
$x$	Solution concentration, kg/kg
$\Delta x$	Solution concentration difference, kg/kg

### Greek symbols

$\varepsilon$	Compressor pressure ratio, dimensionless
---------------	--

### Subscripts

A	Absorber
C	Condenser
E	Evaporator
G	Generator
$opt$	Optimal value
$r$	Refrigerant
$s$	Strong solution

$u$	Ultimate state
$w$	Weak solution

## References

- [1]Y. Fan, L. Luo, B. Souyri, Review of solar sorption refrigeration technologies: development and applications, *Renewable & Sustainable Energy Reviews*, 2007,11: 1758-1775.
- [2]R. Ventas, A. Lecuona, A. Zacarias, M. Venegas, Ammonia-Lithium nitrate absorption chiller with an integrated low-pressure compression booster cycle for low driving temperature, *Applied Thermal Engineering*, 2010, 30: 1351-1359.
- [3]D. Boer, M. Valles and A. Coronas, Performance of double effect absorption compression cycles for air-conditioning using methanol-TEGDME and TFE-TEGDME systems as working pairs, *Int. J. Refrig.*, 1998, 21(7): 542-555.
- [4]Jin-Soo Kim, Felix Ziegler, Huen Lee, Simulation of the compression-assisted triple-effect H<sub>2</sub>O/LiBr absorption cooling cycles, *Applied Thermal Engineering*, 2002,22:295-308.
- [5]Norio Sawada, Kazuaki Minato, Yoshifumi Kunigi, Teiichi Mochizuki, Takao Kashiwagi, Cycle simulation and COP evaluation of absorption-compression hybrid heat pumps: heat amplifier type, *International Absorption Heat Pump Conference ASME*, 1993, 31:471-476.
- [6]Daliang Hong, Limin Tang, Yijian He, Guangming Chen, A novel absorption refrigeration cycle, *Applied Thermal Engineering*, 2010, 30: 2045-2050.
- [7]Guangming Chen, Eiji Hihara, A new absorption refrigeration cycle solar energy, *Solar Energy*, 1999, 66(6): 479-482.
- [8]Wei Han, Liuli Sun, Danxing Zheng, Hongguang Jin, Sijun Ma, Xuye Jing, New hybrid absorption-compression refrigeration system based on cascade use of mid-temperature waste heat, *Applied Energy*, 2013, 106: 383-390.
- [9]Danxing Zheng, Xuelin Meng, Ultimate refrigerating conditions, behavior turning and a thermodynamic analysis for absorption-compression hybrid refrigeration cycle, *Energy Conversion and Management*, 2012, 56: 166-174.
- [10]Xuelin Meng, Danxing Zheng, Jianzhao Wang, Xinru Li, Energy saving mechanism analysis of the absorption-compression hybrid refrigeration cycle, *Renewable Energy*,2013, 57: 43-50.
- [11]Aspen Plus. Aspen Technology, Inc., version 7.3. See also: <http://www.aspentech.com/>.
- [12]J. Patek, J. Klomfar A computationally effective formulation of the thermodynamics properties of LiBr–H<sub>2</sub>O solutions from 273 to 500 K over full composition range *Int. J. Refrig.*, 29 (2006), pp. 566–578.